Comparison of calibration processes of a surface determining measurement system

B. Al-Gaadi
M.Sc. Student, Department of Polymer Engineering, Budapest University of Technology and Economics, H-1111 Budapest, Muegyetem rkp. 3. Tel.: (1) 463-2650, e-mail: byd@freemail.hu

M. Halász
Associate Professor, Department of Polymer Engineering, Budapest University of Technology and Economics, H-1111 Budapest, Muegyetem rkp. 3. Tel.: (1) 463-2650, e-mail: halaszm@pt.bme.hu

L. Szabó
PhD Student, Department of Polymer Engineering, Budapest University of Technology and Economics, H-1111 Budapest, Muegyetem rkp. 3. Tel.: (1) 463-3083, e-mail: szabol@pt.bme.hu

Abstract: *The automatic surface determining device that operates on the optical principle and applies digital image processing methods was developed at BME, primarily for the determination of anthropometrical data but it is also capable of measuring other spatial shape. The advantage of the optical system compared to conventional measuring devices that it is non-touch. The presentation introduces the surface determining device, and then details the applied calibration and measurement evaluation methods: numeric measurement evaluation based on geometry, analytic measurement evaluation based on geometry, calibration with numeric iteration and image evaluation with identification. It also presents the results obtained with the calibration measurements. Based on the results the optimal setting parameters of the measuring device can be determined, and the simple, fast and accurate evaluation of the images taken by the device can also be realized.*

Keywords: apparel industry, body scanner, laser line, calibration

1. INTRODUCTION

The automatic surface determining device that operates on the optical principle and applies digital image processing methods was developed at BME, primarily for the determination of anthropometrical data but it is also capable of measuring other spatial shape. The advantage of the optical system compared to conventional measuring devices that it is non-touch, hence no measuring pressure that would change the shape and no other inconvenient mechanical impact is exerted on the person.

After the surface to be measured is scanned with horizontal laser lines and is photographed with a digital camera at each level the spatial data of the surface can be determined from the photographs with the suitable method based on the calibration. The question is which the sufficient methods of calibration and of the determination of the surface spatial data are. The following 4 different methods have been compared in our work: numeric measurement evaluation based on geometry, analytic measurement evaluation based on geometry, calibration with numeric iteration and image evaluation with identification. The aim of the measurements to be revealed in our presentation is to compare the 4 methods and to evaluate their applicability.

2. MEASUREMENT EQUIPMENT

Fig. 1 illustrates the relative spatial position of the measuring device and the measured surface [3]. During the measurement, the line laser diode in the *X-Y* plane projects a horizontal (parallel with the *X-Z* plane) red light line to the examined surface in front of the

vertical basis plane (*Y-Z* plane), while the CCD camera in the *X-Y* plane takes a digital photograph of the lightened part from a higher position. The light line gives a distorted image – depending on the geometrical arrangement – of the planar section of the surface from the position of the camera [7].
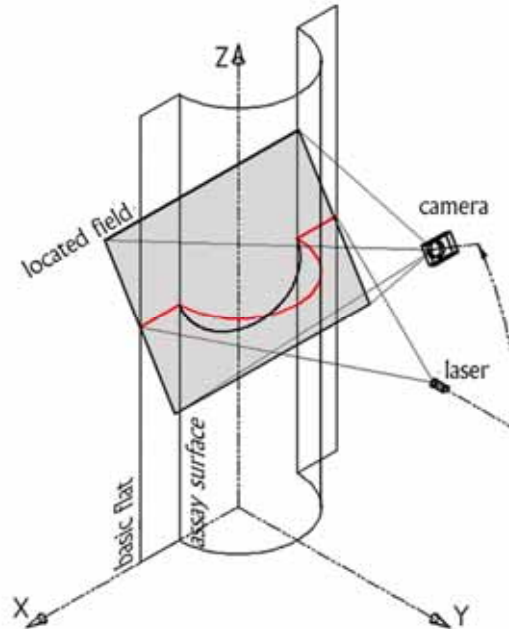
Fig.1. The applied method of light cutting [4]

The image of laser light in the photograph is not a single curve as expected but a band (Fig. 2). The curve that defines the contour of the planar section of the scanned body should be determined from this band. Lajos Szabó [5] worked out a simple, special process for the determination of the points of the curve to be found. If the image is examined, it can be seen that the points of the laser light in the image are in a mostly horizontal band. The essence of the process is that the image is examined perpendicular to the horizontal band pixel column by pixel column. It searches for the pixels in the light band, and then for the brightest pixel within that, and this is considered to be the point of the contour curve to be found.
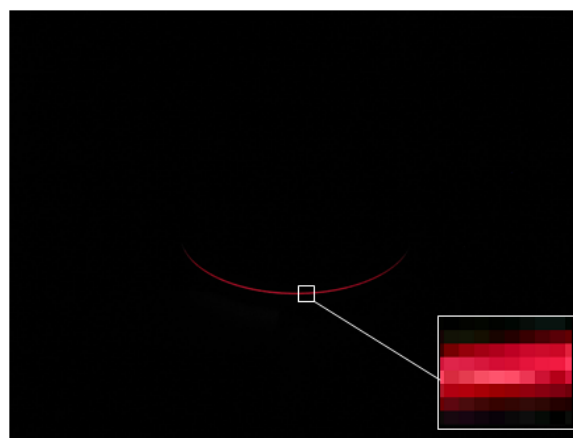
Fig.2. Laser light on the object

After the points of the contour curve are found, the spatial geometrical data of the planar section of the surface determined by the laser line can be determined knowing the

relative position of the basis plane, the camera, the diode and the examined surface. 4 calibration transformation methods compared in order to solve this task.

The calibration transformation methods were compared using 3 special, etalon prisms in the measurements. The etalon prisms are illustrated in Fig. 3.

Square etalon   Semi-circular etalon   Step etalon

Fig.3. Square and step-shaped calibration prism (1., 3.), and semi-circular control prism (2.)

3. METHODS OF CALIBRATION AND MEASUREMENT EVALUATION

The question is how the original position of the surface points can be found out based on the photographs taken during the measurements [1]. The mutually explicit mapping between the photographed plane and the points of the photograph can be described with a non-linear function. In order to be able to define the function explicitly, the parameters of the camera and the accurate relative position of the device and the plane would be necessary. However, these parameters and data cannot be determined easily at the required level of accuracy. 4 different methods compared for the calibration transformation of the applied measuring device are detailed in the following part. The calibration transformations also involve the geometrical transformations used in the measurement evaluation.

3.1. Calibration transformation on analytic geometrical base – Method 1

The geometrical conditions of the measurement are revealed in Fig. 4.

Fig.4. Geometrical relations of the object and the image

Only the geometrical connection between the object and the image are analyzed using the principle of central projection, and the way how the objective produces the image optically on the CCD is not considered. The image is interpreted in a virtual image plane parallel with the CCD of the camera using the principle of central projection (x-y). The intersection point of the axis of the objective and image plane is K, while the center of central projection is C. The real, spatial position of point P is found based on its image, P_k that appears in the image plane.

The geometrical relations are characterized with 3 unknown difficult to measure parameters α, f and l (Fig. 4). Their values can be determined with the help of the square calibration prism.

The calibration square with side d is placed in the object plane (left side of Fig. 5). The etalon image of the square is illustrated in the right side of Fig. 5. The geometrical relation of the calibration is revealed in Fig. 6.
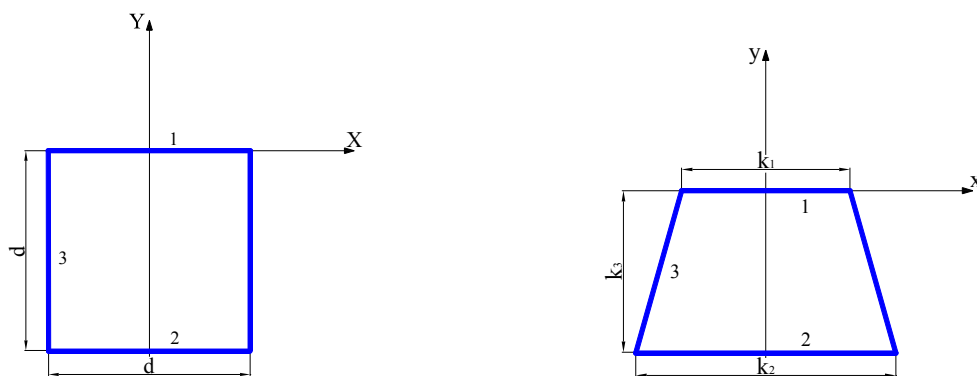
Fig.5. Calibration square in the object and the image plane
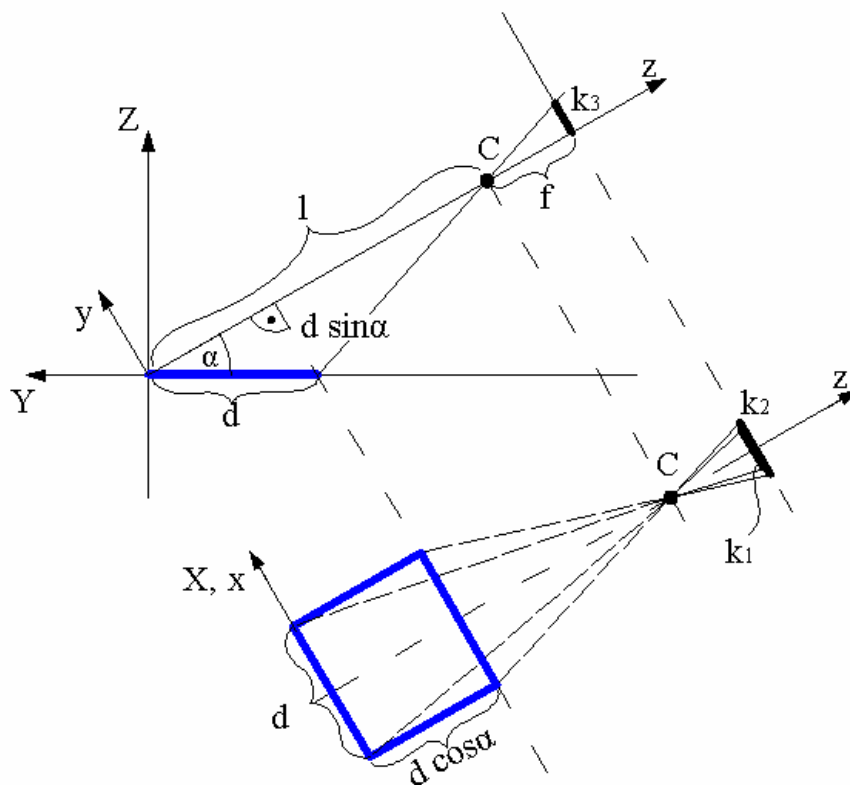
Fig.6. Analytic geometrical calibration

Using the notations of Fig. 6, the calibration parameters can be calculated in the following way (1, 2, 3):

$$\alpha = \arcsin \frac{k_3}{k_2} \tag{1}$$

$$l = d \frac{k_2 \cos \alpha}{k_2 - k_1} \tag{2}$$

$$f = k_1 \frac{k_2 \cos \alpha}{k_2 - k_1} \tag{3}$$

Homogeneous coordinates, coordinate transformation and the principle of central projection were applied when deriving the necessary formula for the determination of the real position of point P (Fig. 4) [2]. As a result of calculation, the following formula, (4) and (5), are obtained for the determination of the real coordinates of point P in the object plane:

$$P_X = \frac{P_{kx} \cdot l \sin \alpha}{f \sin \alpha + P_{ky} \cos \alpha} \tag{4}$$

$$P_Y = \frac{P_{ky} \cdot l}{f \sin \alpha + P_{ky} \cos \alpha} \tag{5}$$

where points P_X and P_Y are the coordinates of point P in the X,Y,Z coordinate system, while P_{kx} and P_{ky} are the coordinates of point P_k in the x,y,z coordinate system.

3.2. Calibration transformation on numeric geometrical base – Method 2

This method makes it possible to describe a mapping between the object plane and the image plane in a way that the relative position of the two planes does not have to be considered [8]. The transformation can be described with a 3x3 matrix using homogeneous coordinates.

The element in the bottom right position is chosen to be 1, and all the others are denoted by m_i ($i=1,\dots8$) out of the 9 elements of the 3x3 matrix $\underline{\underline{M}}$ that describes the transformation. Transformation with the matrix is described with formula (6) below:

$$\begin{bmatrix} x_h \\ y_h \\ z_h \end{bmatrix} = \begin{bmatrix} m_1 & m_2 & m_3 \\ m_4 & m_5 & m_6 \\ m_7 & m_8 & 1 \end{bmatrix} \cdot \begin{bmatrix} x_k \\ y_k \\ z_k \end{bmatrix} \tag{6}$$

where x_h, y_h, z_h are the homogeneous coordinates of the examined point in the object plane, while x_k, y_k, z_k are the homogeneous coordinates of the examined point in the image plane.

If the homogeneous coordinates are computed back to Descartes coordinates, and considering that $z_k=1$, formulae (7) and (8) are obtained for the object plane coordinates:

$$x = \frac{m_1 x_k + m_2 y_k + m_3}{m_7 x_k + m_8 y_k + 1} \tag{7}$$

$$y = \frac{m_4 x_k + m_5 y_k + m_6}{m_7 x_k + m_8 y_k + 1} \tag{8}$$

The elements of the matrix are determined with calibration. If the square etalon is photographed, 4 points are obtained (Fig. 7, corner points of the square etalon) the coordinates of which are known both in the object and in the image plane.
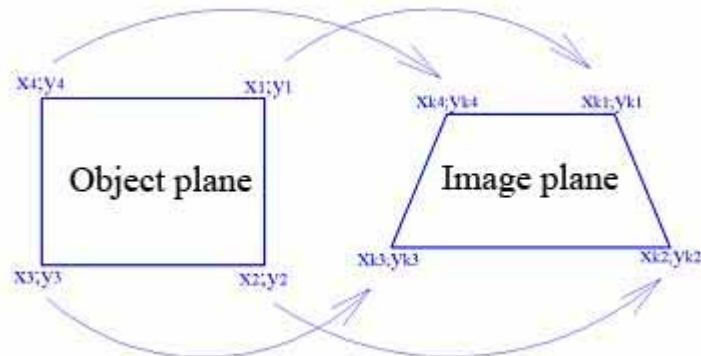
Fig.7. Points in the object plane and their image in the image plane

If these are substituted in equations (7) and (8), a linear equation system with 8 variables is obtained, and its solutions are the elements of the transformation matrix.

3.3. Calibration transformation with iteration – Method 3

Let us suppose again that the real spatial position and the position in the photograph of corner points *A*, *B*, *C* and *D* of the square etalon are all known and origin *O* can be determined by diagonals [6]. The question is how to determine the ζ and η coordinates of an arbitrary point *P* (Fig. 8).

The coordinate axes divide the square into four quarters, and one of those contains point *P*. The corner points of the four quarter squares are known since the *x* coordinate of *C'* is 0, while the *y* coordinate is the same as that of point *B*. Likewise, the *y* coordinate of *A'* is 0, while the *x* coordinate is the same as that of point *A*.

The side of square *A'BC'O* is exactly half of the side of the original *ABCD* square, hence the coordinates of point P can be estimated better than so far (coordinate ζ falls between *A'* and *O*, while coordinate η between *O* and *C'*).

Based on corner points *A'*, *B*, *C'* and *O*, center point *O'* of the new square can be determined if diagonals *A'C'* and *OB* are drawn. With center point *O'* square *A'BC'O* is again divided into four quarters, one of which contains point P and these corner points give a better approximation for the coordinates. The division of squares can be continued. If the division is refined, a better and better estimation can be obtained for the original coordinates, ζ and η. The accurate determination of the position is only limited by the resolution (pixel number) of the photograph.
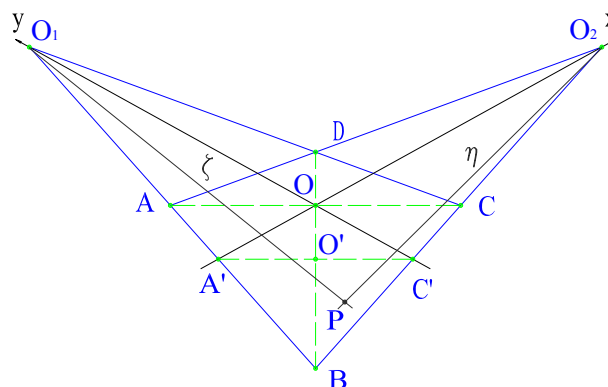
Fig.8. Numerical calibration with iteration

3.4. Calibration transformation with identification – Method 4

A possible way of image evaluation and calibration is when the real points and those in the image plane are correlated in the total measuring zone.

During the measurement, the steps of the special calibration prism were used in a territory 400 mm wide and 200 mm deep in the measuring zone to produce a 10x10 mm virtual grid in a way that the calibration prism was moved with 10 mm, parallel with the base plane, after each image producing phase. A part of the grid formed this way is shown in Fig. 9. Hence all the coordinates of the nods in the grid are known.
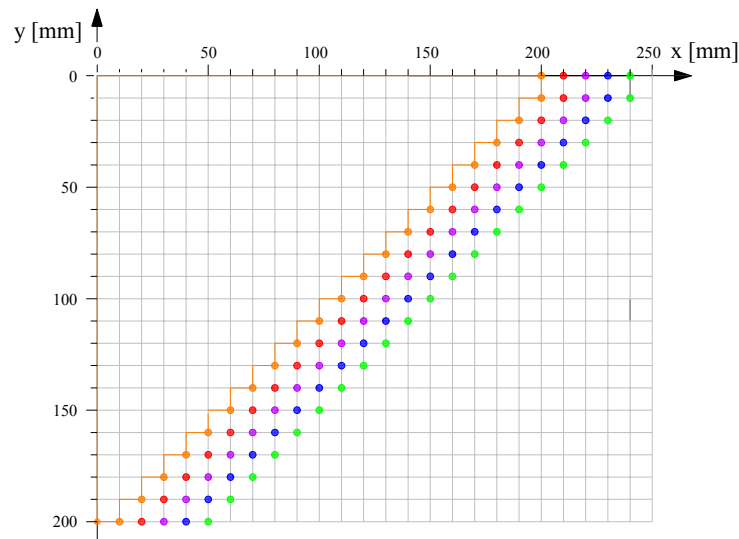
Fig. 9. Corner points of the steps of the calibration prism in the real measurement zone

If the laser line that appears on the calibration prism is photographed in every step. The image of the same grid is distorted due to the perspective and because of the photography the size ratio of the image is also changed. The calibration prism is photographed in different positions shown in Fig. 9, and the corner points of the steps are summarized in one picture, Fig. 10 is obtained.
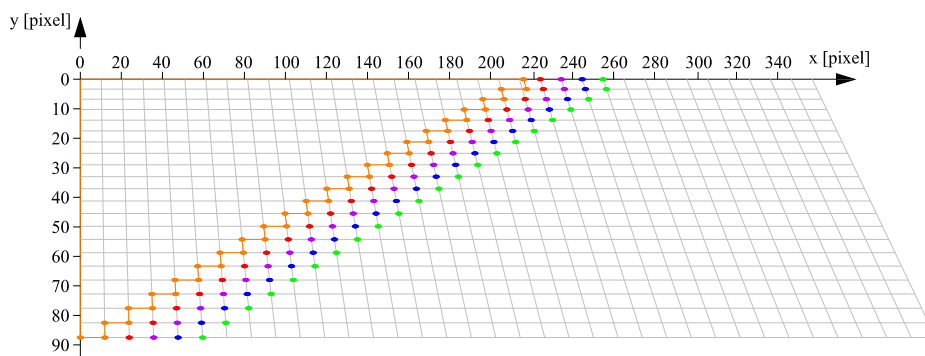
Fig. 10. The coordinates of the steps of the calibration prism measured in the image in pixel

As a result of the measurement, the real *x* and *y* coordinates in mm as well as the x_k and y_k coordinates in the image plane in pixel are assigned to every nod of the 10x10 mm virtual grid.

The coordinates of the points that fall into the nods are obtained automatically. The determination of the coordinates of the points that fall among the nods (Fig. 11) is carried out with linear interpolation using the nearest 4 nods, supposing that the accuracy is sufficient.
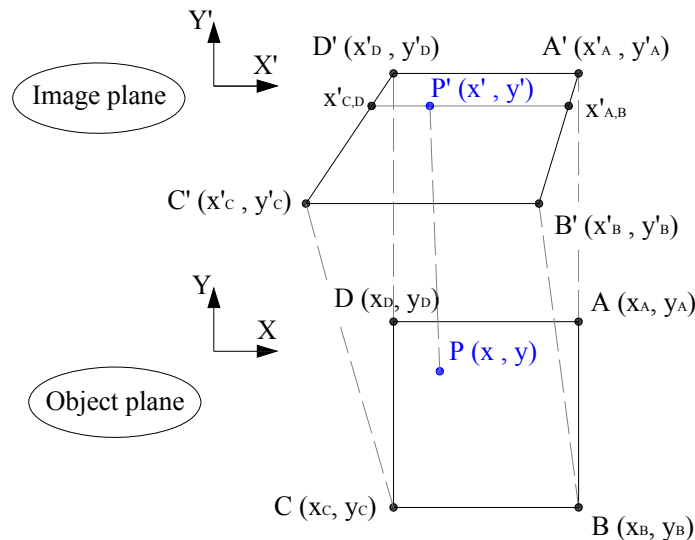
Fig. 11. A 10×10 mm grid square in the object and image plane, notations for the calculation of the real coordinates of point P_k that falls inside the nod square

Using the nearest 4 points, linear interpolation and the notations of Fig. 11, equations (9) and (10) are obtained for the determination of the object plane coordinates of point P.

$$x = \frac{(x'-x'_{A,B}) \cdot (x_D - x_A)}{x'_{C,D} - x'_{A,B}} + x_A \tag{9}$$

$$y = \frac{(y'-y'_A) \cdot (y_B - y_A)}{y'_B - y'_A} + y_A \tag{10}$$

4. THE MEASUREMENT AND THE ANALYSIS OF RESULTS

In order to compare the calibration methods, a semi-circular etalon was used in the measurement. 15 points were selected for the examination from the images taken of the semi-circular etalon (Fig. 2). The real object plane coordinates of the selected 15 points were determined with the methods described in chapter 3.

Fig. 12 illustrates the results obtained with the 4 methods. The 15 points were connected with an approximation curve so that they are easier to compare to the curve drawn in black according to the nominal radius of the semi-circular etalon.

For a more accurate comparison of the calibration transformation methods, a regression process determining size and shape stability was applied. With the help of the regression process the best radius and the best center point of the circle that approximates the 15 points are found, and the deviation of the 15 points from this was examined.
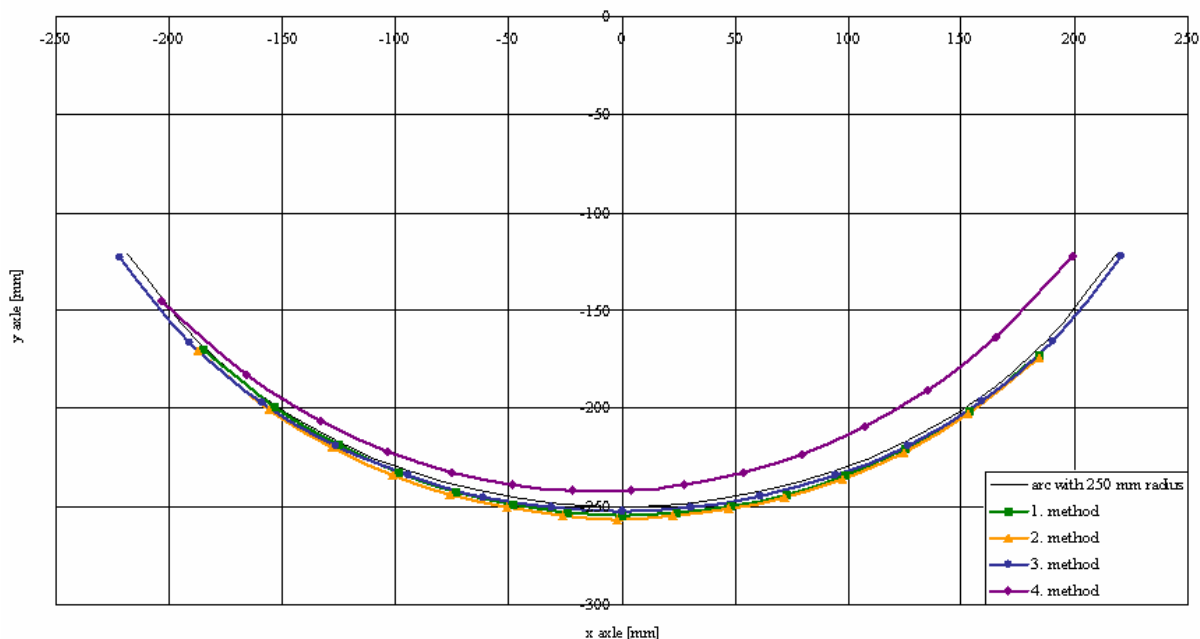
Fig.12. Comparison of the values obtained with the 4 methods

Let the radius of the best approximating circle be *R* and the coordinates of its center point x_0 and y_0. Calculate the distance of the points obtained as a result of our measurements for this center point, and denote this distance with R_i (11).

$$R_i = \sqrt{(x_i - x_0)^2 + (y_i - y_0)^2} \qquad (11)$$

where x_i, y_i, $i=1, \ldots.15$, are the coordinates of the points obtained with the methods.

In order to obtain the radius of the approximating curve and the coordinates of its center point, the minimum of formula (12) below should be determined:

$$\sum_{i=1}^{15} |R_i - R| = \min \qquad (12)$$

To make it computable with a computer, relation (13) equivalent with (12) is used for finding the minimum.

$$\Delta = \sum_{i=1}^{15} \left(R_i^2 - R^2\right)^2 = \min \qquad (13)$$

During the regression calculation the x_0, y_0, R value triple are to be found in case of which *Δ* in formula (13) is minimal. The minimum is searched for with iteration – using the Solver utility of the Excel software – and the initial values were the nominal values listed in Table 1.

x_{0n} [mm]	y_{0n} [mm]	R_n [mm]
0	0	250

Tab.1. Nominal parameters of the examined semi-circle

The results of the calculation are summarized in Table 2, and illustrated in Figs. 13 and 14. *S* in the table denotes the deviation of radius R_i from radius R of the best approximating circle.

Methods	$x_0\text{-}x_{0n}$ [mm]	$y_0\text{-}y_{0n}$ [mm]	R [mm]	$R\text{-}R_n$ [mm]	S [mm]	Δ [mm^2]
Method 1	1.40	-8.09	246.04	-3.96	0.28	270002.65
Method 2	0.14	-7.32	248.38	-1.62	0.25	220175.77
Method 3	-0.50	0.77	253.18	3.18	0.15	83649.78
Method 4	-10.42	-1.67	239.55	-10.45	0.98	3067906.19

Tab.2. Values obtained with regression

Based on the regression size and shape stability analysis, the results obtained with the different methods can be evaluated well. The deviation values and also Fig. 14 reveal that the results of the first three methods are circles with good approximation, i.e. are adequate concerning shape stability. The first three methods are also sufficient concerning size stability since the deviation of the radius of the regression circle and the nominal radius is inside the acceptable range.
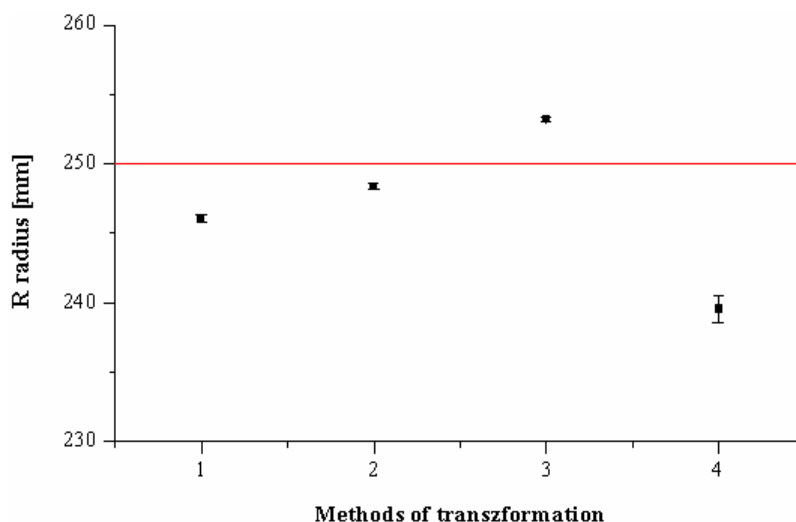
Fig.13. Average and deviation of radius values obtained with regression
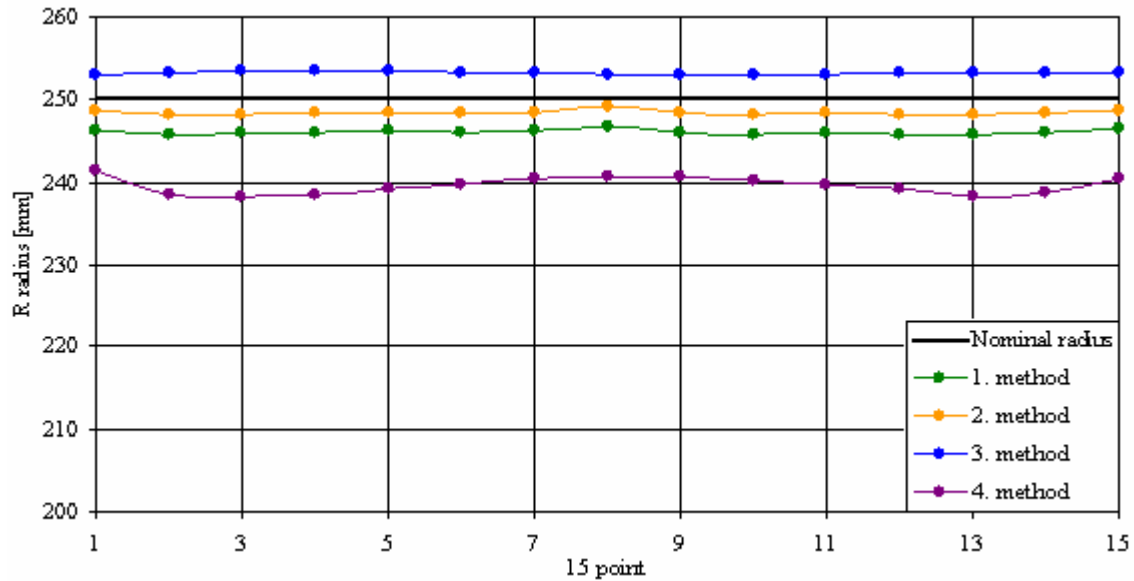
Fig.14. Comparison of values obtained with method 4

Apparently, method 4 gives the results that are farthest from reality. The advantage of this method would be that it is not sensitive to the accuracy of the geometrical setting and eliminates the possible distortions of the optics, since the mapping of the camera is examined in the total measurement range. As opposed to this advantage, the measurements revealed that the drawback is more significant as 4 calibration points are needed in the vicinity for the determination of every single point. A lot of image has to be taken for this purpose, and this is not only much work but also a source of more errors.

The results obtained with method 1 are acceptable concerning both size and shape stability. However, the disadvantage of the method is that the results are strongly influenced by the geometrical position of the camera, the accuracy of its setting and that the simultaneous scanning from more sides cannot be handled easily.

Methods 2 and 3 have given the results that approximate reality the best. Concerning the radius of the regression circle method 2, and concerning the deviation of radii method 3 is the number one. There is a difference in the time necessary for computer processing. From this aspect the numeric geometrical transformation is better due to its faster algorithm than the iteration method. The two methods can both be applied as the calibration transformation process of the surface determining measurement device.

5. SUMMARY

Experiments were carried out with the automatic, surface determining measurement device that operates on the optic principle in order to find the method out of the 4 calibration transformations that is the most suitable for measurement evaluation.

Based on the results it can be stated that the transformation with identification did not turn out to be as good as expected but the other three methods can be used well for solving the task. The drawback of the analytic geometrical method is that it requires a very precise setting of the geometry and the knowledge of the basis plane, and hence is difficult to realize under real measurement conditions. There is only a difference in the speed of computer processing between the numeric geometrical and the iteration method but concerning size and shape stability they both can be applied.

REFERENCES
[1] Al-Gaadi B.: Antropometriai felületbeolvasó mérőrendszer elemzése (Analysis of an anthropometrical surface reading system), BME Diploma Dolgozat, Budapest (2007).
[2] Nagyné dr. Szilvási M.: CAD iskola (CAD school). TipoTEX Kft Elektronikus Kiadó, Budapest (1991).
[3] Szabó L., Halász M.: Line-laser 3D Surface Scanning Machine Planning for the Apparel Industry, in 'Proceeding of GÉPÉSZET 2004 conference, Budapest', 490-494 (2004).
[4] Szabó L., Halász M.: Automatic determination of body surface data, in 'Proceeding of AUTEX 2005 conference, Portorož, Slovenia', 715-720 (2005).
[5] Szabó L., Halász M.: Development of the image post processing of a 3D human body scanner, in 'Proceeding of GÉPÉSZET 2006 conference, Budapest', CD (2006).
[6] Tamás P.: Térbeli ruhatervezés (Spatial apparel design), PhD dissertation, Budapest (2008).
[7] Szabó L.: Képalkotásra alapozott ruhaipari méréstechnikák (Measurements techniques based on image production), BME Phd dissertation, Budapest (2008).
[8] Dong-Keun K., Byung-Tae J.,Chi-Jung H.: A Planar Perspective Image Matching using Point Correspondences and Rectangle-to-Quadrilateral Mapping, in 'Proceeding of Fifth IEEE Southwest Symposium on Image Analysis and Interpretation, Santa Fe, New Mexico', 1532-1537 (2002).